nature genetics

Functional classification of drugs by properties of their pairwise interactions

Pamela Yeh[1], Ariane I Tschumi[1] & Roy Kishony[1,2]

Multidrug treatments are increasingly important in medicine and for probing biological systems[1–6]. Although many studies have focused on interactions between specific drugs, little is known about the system properties of a full drug interaction network[6]. Like their genetic counterparts, two drugs may have no interaction, or they may interact synergistically or antagonistically to increase or suppress their individual effects. Here we use a sensitive bioluminescence technique[7,8] to provide quantitative measurements of pairwise interactions among 21 antibiotics that affect growth rate in *Escherichia coli*. We find that the drug interaction network possesses a special property: it can be separated into classes of drugs such that any two classes interact either purely synergistically or purely antagonistically. These classes correspond directly to the cellular functions affected by the drugs. This network approach provides a new conceptual framework for understanding the functional mechanisms of drugs and their cellular targets and can be applied in systems intractable to mutant screening, biochemistry or microscopy.

Drugs and other small molecules represent alternatives to mutation for exploring the effects of perturbations on biological systems[9]. Much as epistasis among mutations provides a basis for analysis of gene function[10–12], so the interactions among multiple drugs provide a means to understand their mechanisms of action. In analogy to mutations, such epistatic interactions between drugs can be classified into three main types: additive (no interaction), synergistic (demonstrating a larger-than-additive effect) and antagonistic (having a smaller-than-additive effect; **Fig. 1a**)[6,10,13,14]. On the basis of these definitions, a pairwise drug interaction network can be defined and measured within a set of biologically relevant small molecules (**Fig. 1b**).

Networks of epistatic interactions encode valuable functional information[10–12,15,16]. We have shown recently that functional modules in yeast metabolism can be identified purely on the basis of epistasis networks by identifying classes of genes that interact monochromatically; that is, with purely synergistic or purely antagonistic epistatic links between any pair of classes[16]. This classification scheme was implemented using the Prism algorithm (**Fig. 1b–f**)[16]. Here, we build on this approach and on the fact that drugs within the same functional

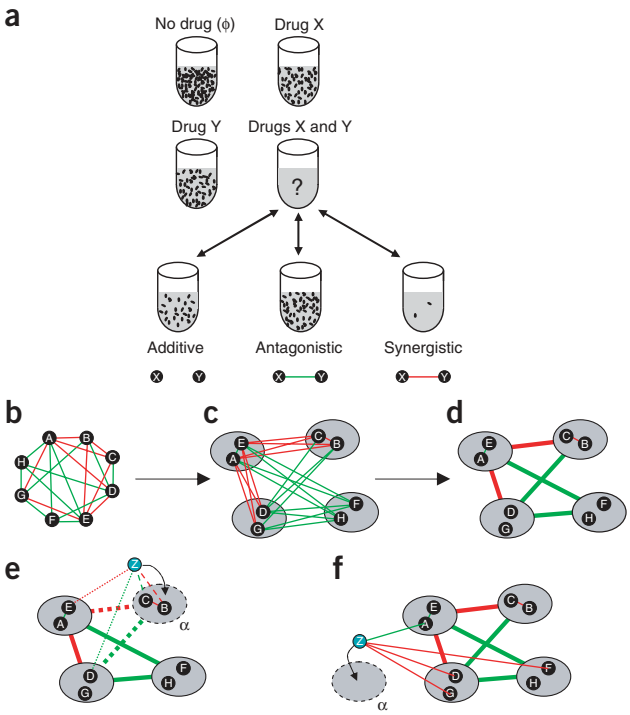

Figure 1 Clustering of individual drugs into functional classes solely on the basis of properties of their mutual interaction network. (**a**) Schematic illustration of additive, synergistic and antagonistic interactions between drugs X and Y by measurements of bacterial growth under the following conditions: no drugs, drug X only, drug Y only, and both drugs X and Y. (**b–d**) A network (**b**) of synergistic interactions (red lines) and antagonistic interactions (green lines) between drugs (black circles) can be clustered into functional classes that interact with each other monochromatically (that is, with purely synergistic or purely antagonistic interactions between any two classes; **c**). This classification generates a system-level perspective of the drug network (**d**). (**e**,**f**) Two independent observations indicate whether a new drug (Z) will be clustered into a particular drug class (α, dashed oval): mixed synergistic and antagonistic intraclass interactions of Z with α (**e**, thin dotted green and red lines) and nonconflicting interclass interactions of Z (**e**, dotted thin lines) and α (**e**, dotted thick lines) with all other classes. Both intra- and interclass indications are depicted in **e**, and the drug is clustered (black arrow) with an existing class. If drug Z has no such intra- or interclass association with any existing drug class, the drug will be clustered in a new class (**f**).

[1]Bauer Center for Genomics Research, Harvard University, 7 Divinity Avenue, Cambridge, Massachusetts 02138, USA. [2]Department of Systems Biology, Harvard Medical School, 240 Longwood Avenue, Boston, Massachusetts 02115, USA. Correspondence should be addressed to R.K. (rkishony@cgr.harvard.edu).

Received 9 November 2005; accepted 26 January 2006; published online 19 March 2006; doi:10.1038/ng1755

Table 1 List of all drugs used in the study, abbreviation, dose used and mechanism of action

Drug	Drug abbreviation	Dose (μg ml^{-1})	Main mechanism(s) of action	Mechanism abbreviation
Chloramphenicol	CHL	1	Protein synthesis, 50S	R
Clindamycin	CLI	4	Protein synthesis, 50S	R
Erythromycin	ERY	4	Protein synthesis, 50S	R
Spiramycin	SPR	20	Protein synthesis, 50S	R
Fusidic acid	FUS	40	Protein synthesis, 50S	R
Amikacin	AMK	20	Aminoglycoside, protein synthesis, 30S	A
Tobramycin	TOB	0.9	Aminoglycoside, protein synthesis, 30S	A
Streptomycin	STR	5	Aminoglycoside, protein synthesis, 30S	A
Tetracycline	TET	2	Protein synthesis, 30S	R
Doxycycline hyclate	DOX	1	Protein synthesis, 30S	R
Spectinomycin	SPX	9	Protein synthesis, 30S	R
Piperacillin	PIP	0.8	Cell wall	W
Ampicillin	AMP	5	Cell wall	W
Cefoxitin	FOX	0.8	Cell wall	W
Nalidixic acid	NAL	2	DNA gyrase	D
Lomefloxacin	LOM	0.07	DNA gyrase	D
Ciprofloxacin	CPR	0.006	DNA gyrase	D
Bleomycin	BLM	5	Nucleic acid, anticancer drug	B
Sulfamonomethoxine	SLF	0.1	Folic acid biosynthesis	F
Trimethoprim	TMP	0.5	Folic acid biosynthesis	F
Nitrofurantoin	NIT	0.3	Multiple mechanisms	M

category often interact with other drugs in similar ways[17], and we develop a new conceptual framework for understanding functional classification of drugs in drug-drug interaction networks. We first describe the experimental system we used to quantitatively measure epistasis among pairs of drugs. We then apply a computational analysis approach to classify the resulting interaction network into monochromatically interacting classes. Finally, we examine implications of the approach for identifying mechanisms of drug action.

We selected 21 antibiotics that cover a wide range of mechanisms of action, including drugs that target cell wall synthesis, nucleic acid synthesis, protein synthesis and folic acid synthesis (**Table 1**)[18,19]. We also included the anticancer drug bleomycin. To quantify epistasis experimentally, we systematically measured the effects of pairs of antibiotics on the growth rate of *E. coli*. We used a bioluminescence assay that allows accurate measurements of bacterial growth rates with a sensitivity exceeding that of standard optical density techniques by three orders of magnitude (**Supplementary Fig. 1** online)[7,8].

To measure drug interactions, we first needed to determine appropriate concentrations for each single drug. In medical research, emphasis is usually placed on high concentrations of antibiotics, above the minimum inhibitory concentrations[19]. Here, we chose to focus on sublethal concentrations of drugs[20] because they provide a direct analogy to mutations used in genetic epistasis studies and because such small perturbations are potentially more reflective of the physiology of the wild-type bacterial state. For each single antibiotic, we measured a dose-response curve (**Supplementary Fig. 2** online) to find a nonlethal concentration at which the effect on growth rate was small but measurable, normally 50–90% of the growth rate in the absence of drugs. (A few drugs, including novobiocin and rifampicin, did not show clear nonlethal effects

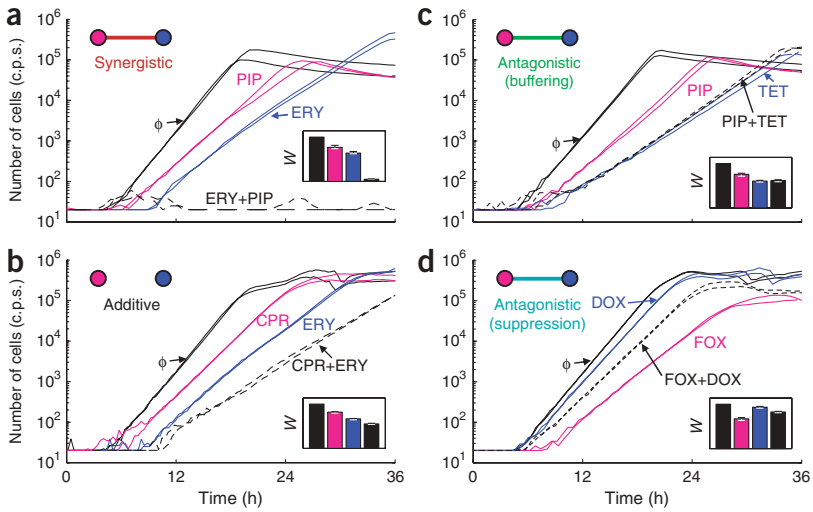

Figure 2 Experimental classification of drug interactions into four types using bioluminescence measurements of bacterial growth in the presence of sublethal concentrations of antibiotics. The pairs of antibiotics illustrate synergistic (**a**), additive (**b**), antagonistic buffering (**c**) and antagonistic suppression (**d**) interactions (see **Table 1** for drug abbreviations). The number of bacteria (proportional to bioluminescence counts per second (c.p.s)[8]) is shown from two replicates, for control with no drugs (ϕ, solid black lines), each single drug (X, Y; blue and magenta lines) and the double-drug combination (X + Y, dashed black lines). Insets: normalized growth rates (*W*) with error bars for ϕ, X, Y and X+Y, from left to right, respectively. Note the contrast between the interactions of piperacillin with the 50S ribosomal subunit drug erythromycin (**a**, ERY-PIP, synergistic) and the 30S ribosomal subunit drug tetracycline (**c**, TET-PIP, antagonistic).

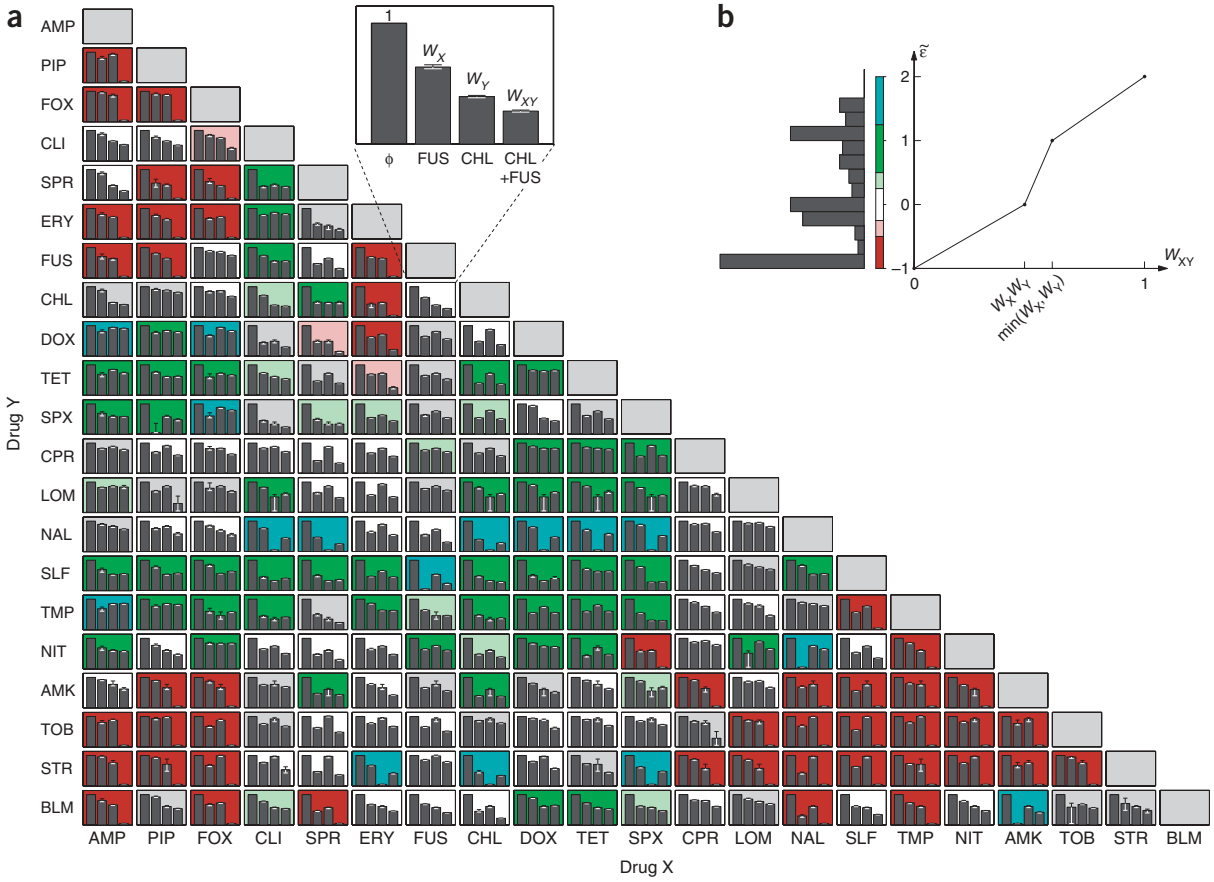

Figure 3 Systematic measurements of pairwise interactions between antibiotics. (**a**) Growth measurements and classification of interaction for all pairwise combinations of drugs X and Y (see **Table 1** for drug abbreviations). Within each panel, the bars represent measured growth rates for, from left to right: no drugs (ϕ), drug X only, drug Y only and the combination of the two drugs X and Y (see inset). Error bars represent variability in replicate measurements (see Methods). The background color of each graph designates the form of epistasis according to the scale in **b**: synergistic (red: $\tilde{\varepsilon}_{max} < -0.5$; pink: $-0.5 < \tilde{\varepsilon}_{max} < -0.25$), antagonistic buffering (green: $0.5 < \tilde{\varepsilon}_{min} < 1.15$; light green: $0.25 < \tilde{\varepsilon}_{min} < 0.5$), antagonistic suppression (blue: $\tilde{\varepsilon}_{min} > 1.15$) or additive (white: $-0.25 < \tilde{\varepsilon}_{max} < 0.5$ and $-0.5 < \tilde{\varepsilon}_{min} < 0.25$). Cases that do not fall into any of these categories are labeled inconclusive (gray background). $\tilde{\varepsilon}_{min}$ and $\tilde{\varepsilon}_{max}$ define our confidence interval for $\tilde{\varepsilon}$ (Methods). (**b**) Graphic representation defining the epistasis interaction scale $\tilde{\varepsilon}$ (W_{XY}, W_X, W_Y) as a function of the normalized growth rate under the double-drug combination (W_{XY}) and the two single drugs (W_X, W_Y)[16]. The histogram of $\tilde{\varepsilon}$ over all drug pairs (at left) shows a trimodal distribution of interactions, with antagonistic, additive and synergistic modes.

on growth rate and were therefore excluded from the study; see **Supplementary Fig. 2**.)

Having chosen effective nonlethal concentrations for each drug, we then conducted pairwise interaction experiments (see **Supplementary Note** and **Supplementary Fig. 3** online for dosage dependence epistasis). For each pair of drugs, we set up, in parallel and on the same microtiter plate, four types of samples, all containing the same *E. coli* strain: control wells with no antibiotics, wells containing each of the two antibiotics individually and wells with the two antibiotics combined. This allowed for comparisons, within parallel experiments, of the normalized reduced growth rate caused by the two antibiotics ($W_{XY} = g_{XY} / g_\phi$), where g_{XY} and g_ϕ are the measured growth rates with two antibiotics and with no antibiotics, respectively, versus that of each of the single antibiotics ($W_X = g_X / g_\phi$, $W_Y = g_Y / g_\phi$). Within each experimental set, we examined all pairwise interactions in at least two replicates. Furthermore, we conducted several independent experimental replicates on different days for each pair of drugs.

The results allowed us to categorize drug interactions into four types: additive, synergistic, antagonistic buffering and antagonistic suppression (see examples in **Fig. 2** and the complete data set in **Fig. 3a**). We define additivity according to Bliss[14]: two drugs are considered additive if the relative phenotypic effect of each of the drugs does not depend on the presence of the other drug ($W_{XY} = W_X W_Y$). We use this definition of additivity because of its simplicity and, more importantly, because it provides an exact analogy to the definition of epistasis conventionally used for genetic perturbations[10,14] (for an alternative definition, see ref. 13). Deviations from additivity are denoted by $\tilde{\varepsilon}$ and are quantified using the following scale: $\tilde{\varepsilon} = (W_{XY} - W_X W_Y) / |\tilde{W}_{XY} - W_X W_Y|$, where $\tilde{W}_{XY} = \min[W_X, W_Y]$ for $W_{XY} > W_X W_Y$ and is 0 otherwise[16]. For $W_{XY} > \min[W_X, W_Y]$, $\tilde{\varepsilon} = (W_{XY} - \min[W_X, W_Y]) / (1 - \min[W_X, W_Y]) + 1$. This scale was introduced in ref. 16; here we extend the definition of $\tilde{\varepsilon}$ to account for suppressing interactions as well (see complete definition in **Fig. 3b**). On the $\tilde{\varepsilon}$ scale, synthetic lethal interactions (that is, no growth during exposure to double-drug combinations ($W_{XY} = 0$, **Fig. 2a**) are mapped to $\tilde{\varepsilon} = -1$; additive interactions ($W_{XY} = W_X W_Y$, **Fig. 2b**) are mapped to $\tilde{\varepsilon} = 0$; antagonistic buffering, when one drug completely masks the effect of the other ($W_{XY} = \min[W_X, W_Y]$, **Fig. 2c**), is mapped to $\tilde{\varepsilon} = 1$; antagonistic suppression, when the combination of drugs yields a higher growth rate than at least one of

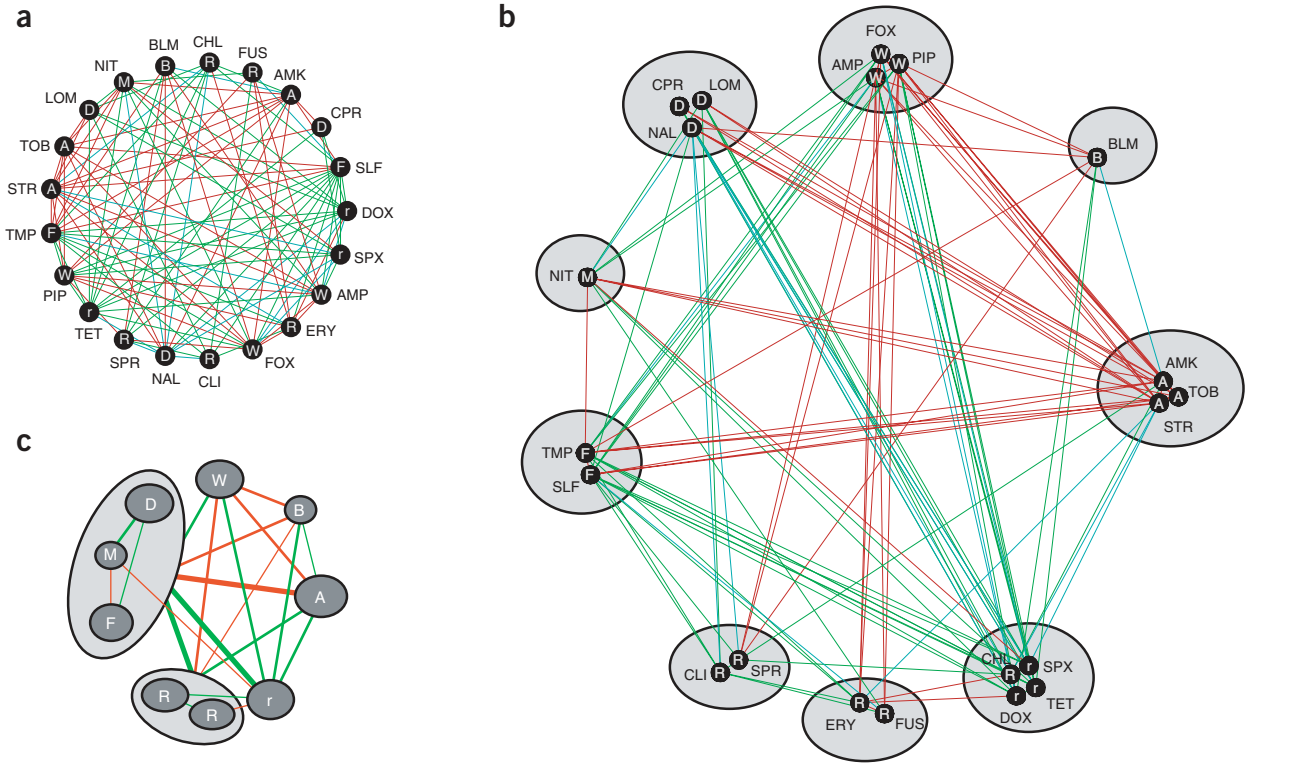

Figure 4 Unsupervised classification of the antibiotic network into monochromatically interacting classes of drugs with similar mechanisms of action. (**a**) The unclustered network of drug-drug interactions with synergistic (red), antagonistic buffering (green) and antagonistic suppression (blue) links. (**b**) Prism algorithm classification of drugs into monochromatically interacting functional classes. This unsupervised clustering shows good agreement with known functional mechanism of the drugs (single letter inside each node; see **Table 1**). Bleomycin (BLM), which is believed to affect DNA synthesis, although its mechanism is not well understood, cannot be clustered monochromatically with any other class. The multifunctional drug nitrofurantoin (NIT) shows non-monochromatic interactions. (**c**) System-level interactions between the drug classes defined in **b**. Larger ellipses show higher-level classification of DNA gyrase inhibitors (D) with inhibitors of biosynthesis of DNA precursors (F) and classification of the two subclasses of drugs involved in the inhibition of protein synthesis via the 50S ribosomal subunit (R).

the single drugs by itself ($W_{XY} > \min[W_X, W_Y]$, **Fig. 2d**), corresponds to $\tilde{\varepsilon} > 1$; and the extreme case of complete recovery of growth ($W_{XY} = 1$) maps to $\tilde{\varepsilon} = 2$. In agreement with theoretical predictions[16], we found that the distribution of $\tilde{\varepsilon}$ is trimodal, allowing a relatively clear separation between synergistic, additive and antagonistic modes (**Fig. 3b**).

To represent the interaction data as a network (**Fig. 4a**), we calculated the value of $\tilde{\varepsilon}$ and its confidence interval ($\tilde{\varepsilon}_{min}$, $\tilde{\varepsilon}_{max}$; see Methods) for each pair and applied the following thresholds: for $\tilde{\varepsilon}_{max} < -0.5$, the interaction is considered synergistic; for $\tilde{\varepsilon}_{min} > 0.5$, antagonistic; otherwise, the interaction is scored as additive. Our results were not very sensitive to these thresholds (**Supplementary Note**). Cases that were inconclusive within the measurement error were categorized as undetermined. We then applied the Prism algorithm (see Methods and ref. 16) to classify the drugs, on the basis of the similarity in their interaction with other drugs, into subclasses that interact with each other monochromatically (**Fig. 4b**). To determine the placement of a drug, Z, into a specific class, α, two independent observations are used. First, if Z interacts both antagonistically and synergistically with drugs in α, Z must be placed in class α to avoid violation of monochromaticity (intraclass; **Fig. 1e**). Second, to be placed in class α, all interactions of Z with all other classes must not conflict with the interactions of α with all other classes. Otherwise, the new drug will cluster by itself; that is, start a new class (**Fig. 1f**). If these two rules are conflicting, such that one rule dictates inclusion in a cluster, and the other rules dictates exclusion, then the drug will have non-monochromatic interactions. In that case, the algorithm will place the drug in a cluster that minimizes the total number of such non-monochromatic links (see nitrofurantoin in **Fig. 4b**).

We found that the individual drugs can be clustered almost perfectly into monochromatically interacting classes (with one notable exception, to be discussed below). This mathematical property is very rare in random networks ($P < 10^{-3}$; **Supplementary Fig. 4** online). Notably, the resulting monochromatically interacting classes correspond strongly with the putative function of the drugs (**Fig. 4b**). For example, the two folic acid biosynthesis inhibitors, sulfamonomethoxine and trimethoprim, cluster together. Similarly, drugs affecting the cell wall cluster together, as do the aminoglycosides and DNA gyrase inhibitor drugs. The protein synthesis drugs, however, do not cluster in a single class: rather, the classification of these drugs reflects a separation into 50S and 30S ribosomal subunit inhibitors. This separation results from different types of interaction that these subclasses show with the cell-wall synthesis inhibitor class[21]. We found that although 50S drugs interact antagonistically with cell-wall drugs, 30S drugs interact synergistically (also compare **Fig. 2a** with **Fig. 2c**). The only exception to this separation is chloramphenicol, which affects the 50S subunit but clusters with the 30S class (note that chloramphenicol showed neither antagonistic nor synergistic interaction with the cell wall drug class).

In general, drug-drug interactions may be of a chemical nature—competition for the same binding site, for example—or may have a genetic basis, reflecting functional connections between target genes. We find that the Prism classification reflects mostly cellular function rather than chemical structure. A good example of this is spectinomycin, which is structurally an aminoglycoside[18] but clustered with the 30S drugs in accordance with its function. This highlights the power of drug interaction networks to reflect true biological function.

The classification of drugs into monochromatically interacting classes allows us to extend the notion of epistatic interactions from the level of individual drug-drug interactions to the level of interactions between functional classes (**Fig. 4c**). Some of these class-class interactions are well known and documented, such as the synergy between the aminoglycoside and cell-wall drug classes[18]. Others are less well known and to our knowledge have not been previously identified, such as the difference in interaction between the two protein synthesis classes, 50S and 30S, with cell wall drugs. A higher-level step in the hierarchical Prism classification is the clustering of the DNA gyrase inhibitors and the folic acid inhibitors (**Fig. 4c**). This is likely to reflect the fact that folic acid biosynthesis is required for DNA synthesis. Another higher-level classification is the clustering of the two classes affecting the 50S subunit in protein synthesis (**Fig. 4c**). This high-level step is not fully monochromatic but is nevertheless still performed by Prism (see Methods for explanation of how Prism deals with non-monochromatic interactions).

Network analysis can also be used to uncover drugs with multiple functions, and this is highlighted by nitrofurantoin, which does not exhibit monochromaticity. This is a particularly interesting exception to monochromaticity because nitrofurantoin, unlike most other drugs in the network, is a synthetic drug that acts on more than one pathway—it affects DNA synthesis, protein synthesis and cell wall synthesis[18]. The multifunctionality of nitrofurantoin is probably the reason why it cannot be clustered monochromatically in the network. Thus, an unanticipated feature of this drug interaction network method is that it is likely to detect multifunctionality. A generalization of this case may suggest a way to screen for drugs with multiple modes of action, although there may be other explanations for non-monochromatic interactions, including differences in metabolism of the drug or existence of specific resistance mechanisms[17].

Another potential use of our approach is to identify drugs with novel mechanisms of action, which can be identified because they cannot cluster monochromatically with any other functional class. We tested a drug whose functional mechanism is less well understood: the anticancer antibiotic bleomycin, which suppresses growth of *E. coli* presumably through oxidation and degradation of DNA[22]. Notably, we found that bleomycin did not cluster monochromatically with any of the other drug classes (**Fig. 4b**). Furthermore, unlike nitrofurantoin, bleomycin showed only monochromatic interactions within any one class, indicating the drug did not need to be clustered within any existing class (see **Fig. 1e**). These two observations require that bleomycin be clustered as a separate functional class. The fact that bleomycin is clustered by itself highlights one of the potentially powerful aspects of this conceptual framework: it may allow rapid screening for drugs that are not only potent but that work through a novel mechanism of action.

We provide a complete and systematic analysis of a drug-drug interaction network. Systems analysis of the interaction network demonstrates that drugs can be classified according to their action mechanism based on their interactions with other functional drug classes. The ability to classify drug function based solely on phenotypic measurements and without the tools of biochemistry or microscopy[21,23,24] can provide a simple and powerful method for screening new drugs with multiple or novel mechanisms of action. Our systems approach is general in nature and could be applied to other biological systems. It would be particularly useful if the approach could be generalized to *in vivo* studies and to a wider range of phenotypes despite added complexity of host-drug interaction. Furthermore, applying network approaches[25–27] to drug interactions may help suggest new drug combinations and highlight the importance of gene-environment interactions[28], including, in particular, the resistance and persistence of bacteria to antibiotics[1,4,5,29] and of cancer cells to antitumor drugs[30].

METHODS

Bacterial strains and growth conditions. Plasmid pCS-λ[7,8], expressing the lux operon from a constitutive lambda promoter, was transformed into a wild-type MG1655 strain. Growth medium was M63 minimal medium supplemented with 0.2% glucose, 0.01% CAS amino acids, 0.5 μg ml^{-1} thiamine. Single-colony transformants were grown to $OD_{600} = 0.6$ at 30 °C with shaking. Cell stocks were prepared at concentrations of 10^5 cells ml^{-1} and stored in multiple aliquots with 15% glycerol at −80 °C.

Growth rate assay. We measured bacterial growth rate using a recently developed bioluminescence technique that allows highly accurate measurements of bacterial densities versus time over three to four orders of magnitude of dynamic range[8]. The measurement is based on bioluminescence photon counting from growing cultures. As we only use the slope to determine growth rates, our values are do not depend on possible changes in the luminescence intensity per cell that could be caused by the antibiotic treatments. The assay was done in 96-well plates (Costar) sealed with clear adhesive tape (Perkin-Elmer) using the Perkin-Elmer TopCount NXT Microplate Scintillation and Luminescence Counter. The reader was kept in a 30 °C room with 70% relative humidity, and readings were acquired with a 1-s integration time per well. For each set of experiments, we ran 10–14 plates in parallel, resulting in each plate being read approximately once every 30–40 min. Plates were cycled in the TopCount for 48–96 h. To eliminate minor spatial temperature gradients across the plates, we used a ventilation scheme around the 96-well plate towers (see **Supplementary Fig. 1** for plate uniformity). Wells were filled with 100 μl growth medium and inoculated with a fresh −80 °C cell stock aliquot diluted 1:1,000 (corresponding to a density of ten cells per well). Log of the measured counts minus the photodetector background (20 counts per second (c.p.s.)) were plotted and analyzed using Matlab. Numerical values for growth rates (g) were obtained by the slope of the line of best fit passing through the data in the exponential region (typically between 5×10^2 and 5×10^3 c.p.s.). Any well that did not have growth after the wild-type wells had undergone 30 cell cycles (approximately 48 h after start of experiment) was considered dead ($g = 0$).

Determining single-drug concentrations. We tested a range of concentrations for each drug, typically 11 different concentrations with twofold intervals (**Supplementary Fig. 2**). We preserved 1–2 ml 10× −20 °C stock of all drug concentrations in M63 media to allow for accurate replication of the concentrations in the subsequent two-drug experiments. For each drug, we chose the concentration that reduced growth rate by a nonlethal but substantial effect relative to the no-drug control (typically 10–50% reduction in growth rate; however, suppression interactions were often better resolved in larger single effects). See the **Supplementary Note** for a discussion of dose dependence.

Drug interaction assay. To measure the combined effect of two drugs versus their individual effects, we filled wells with 100 μl total medium consisting of 80 μl of growth medium inoculated with 1:1,000 of our −80 °C bacterial cell stock and one of the following four options: (i) 20 μl of M63 media only, for control; (ii) 10 μl of M63 media only and 10 μl 10× stock of drug X (in M63 media), to measure the growth rate of X singly; (iii) the same for drug Y; or (iv) 10 μl 10× stock of drug X and 10 μl of 10× stock of drug Y, to measure the two-drug growth rate. We tried to keep the single-drug concentration of each drug fixed for all of its pairwise combinations, which often required fine-tuning of

dosages. The concentration (as evidenced by the single-drug wells) of some of the drugs was not always constant across all experiments, especially for drugs with high sensitivity to dosage (see, for example, piperacillin in **Supplementary Fig. 2**).

Classification of drug interactions. To characterize epistatic effects between pairs of drugs, we compared the effects of each double-drug combination with those of the corresponding single drugs at the same dose, measured in parallel and on the same plate. Multiple well replicates ($\sim$100 for no drugs, $\sim$16 for each single drug and at least two for the double-drug combination) were conducted for each growth condition C (that is, for no drugs, C = ϕ; for single drugs, C = X or Y; for both drugs, C = XY). For each well (i) in growth condition C we measured the growth rate (g_C^i) and normalized it to the average growth rate g_ϕ of the no-drug control, $W_C^i = g_C^i/g_\phi$. We defined W_C, $W_C^{\min}$ and $W_C^{\max}$ as the median, 10th and 90th percentiles over i of W_C^i, respectively. When there were fewer than ten well replicates, we defined $W_C^{\min}$ and $W_C^{\max}$ as the minimal and maximal values over all measurements. As the variability of small statistical samples may not correctly reflect the actual variability in the data, we assumed a minimum of 2% error (**Supplementary Fig. 1**) in cases in which the replicate variability was smaller. For each drug pair X and Y, we define the median epistasis value $\tilde{\varepsilon}_{XY} = \tilde{\varepsilon}(W_{XY},W_X,W_Y)$, where the function $\tilde{\varepsilon}(W_{XY},W_X,W_Y)$ is defined in **Figure 3b**. We further defined the confidence interval for $\tilde{\varepsilon}$ as

$$\tilde{\varepsilon}_{\min} = \min_{w_{XY},w_X,w_Y} \tilde{\varepsilon}(w_{XY}, w_X, w_Y)$$

and

$$\tilde{\varepsilon}_{\max} = \max_{w_{XY},w_X,w_Y} \tilde{\varepsilon}(w_{XY}, w_X, w_Y),$$

where w_{XY}, w_X and w_Y range within their respective confidence intervals defined above. The difference $\tilde{\varepsilon}_{\max} - \tilde{\varepsilon}_{\min}$ reflects the quality of the experiment and was used to choose a good experimental replicate for a particular drug pair. The interaction was considered antagonistic if $\tilde{\varepsilon}_{\min} > 0.5$ and synergistic if $\tilde{\varepsilon}_{\max} < -0.5$.

The Prism algorithm. The original Prism algorithm[16] is designed to cluster networks into purely monochromatic classes. This algorithm, however, is not particularity suited for dealing with networks that cannot be clustered purely monochromatically or with measurement errors and variability. We have therefore constructed a new version of the algorithm, PrismII, in which monochromaticity is not strictly enforced but is instead accounted for as an entropy cost term. We start with each drug assigned into a distinct cluster. In sequential clustering steps, the pairs of clusters (x, y) with minimal distance are combined until the whole network is clustered into a single class. The distance $F_{x,y}$ between clusters x and y is calculated as

$$F_{x,y} = \min_{X\in x, Y\in y} \{e_{X,Y}\} - T\Delta S_{x,y},$$

with the Euclidean distance

$$e_{X,Y} = \frac{1}{4N}\sum_{Z=1}^{N} (\tilde{\varepsilon}_{X,Z} - \tilde{\varepsilon}_{Y,Z})^2$$

and a monochromaticity entropy term:

$$\Delta S_{x,y} = S(\mathbf{m}_{x,y}) - \sum_{z\neq x,y} [S(\mathbf{m}_{x,z} + \mathbf{m}_{y,z}) - S(\mathbf{m}_{x,z}) - S(\mathbf{m}_{y,z})].$$

$\mathbf{m}_{x,y} = \{m_{x,y}^-, m_{x,y}^+\}$ is a vector containing the number of synergistic (–) and antagonistic (+) links between clusters x and y. The entropy function is defined by

$$S(\mathbf{m}) = (m^+ + m^-)(p^+ \log p^+ + p^- \log p^-),$$

where $p^{+/-} = m^{+/-}/(m^+ + m^-)$. T is a free parameter and was set to 0.1 in our analysis. Twofold variations in T gave similar results.

Note: Supplementary information is available on the Nature Genetics website.

ACKNOWLEDGMENTS

We thank N. Barkai, J. Clardy, A. De Luna, M. Elowitz, L. Garwin, M. Hegreness, H. Hofmann, D. Kahne, G. Lahav, M. Laub, T. Mitchison, A. Murray, E. O'Shea, S. Renn, V. Savage, D. Segrè, N. Shoresh and C. Walsh for helpful suggestions and for comments on the manuscript. We acknowledge support from the Bauer Center for Genomics Research.

COMPETING INTERESTS STATEMENT

The authors declare that they have no competing financial interests.

Published online at http://www.nature.com/naturegenetics
Reprints and permissions information is available online at http://npg.nature.com/reprintsandpermissions/

1. Walsh, C. Molecular mechanisms that confer antibacterial drug resistance. *Nature* **406**, 775–781 (2000).
2. Hurley, L.H. DNA and its associated processes as targets for cancer therapy. *Nat. Rev. Cancer* **2**, 188–200 (2002).
3. Leeb, M. Antibiotics: a shot in the arm. *Nature* **431**, 892–893 (2004).
4. Levy, S.B. & Marshall, B. Antibacterial resistance worldwide: causes, challenges and responses. *Nat. Med.* **10**, S122–S129 (2004).
5. Nathan, C. Antibiotics at the crossroads. *Nature* **431**, 899–902 (2004).
6. Keith, C.T., Borisy, A.A. & Stockwell, B.R. Multicomponent therapeutics for networked systems. *Nat. Rev. Drug Discov.* **4**, 71–78 (2005).
7. Bjarnason, J., Southward, C.M. & Surette, M.G. Genomic profiling of iron-responsive genes in *Salmonella enterica* serovar typhimurium by high-throughput screening of a random promoter library. *J. Bacteriol.* **185**, 4973–4982 (2003).
8. Kishony, R. & Leibler, S. Environmental stresses can alleviate the average deleterious effect of mutations. *J. Biol.* **2**, 14 (2003).
9. Schreiber, S.L. The small-molecule approach to biology. *Chem. Eng. News* **81**, 51–61 (2003).
10. Hartman, J.L., Garvik, B. & Hartwell, L. Cell biology - Principles for the buffering of genetic variation. *Science* **291**, 1001–1004 (2001).
11. Tong, A.H. *et al.* Global mapping of the yeast genetic interaction network. *Science* **303**, 808–813 (2004).
12. Davierwala, A.P. *et al.* The synthetic genetic interaction spectrum of essential genes. *Nat. Genet.* **37**, 1147–1152 (2005).
13. Loewe, S. The problem of synergism and antagonism of combined drugs. *Arzneimittel-Forschung-Drug Research* **3**, 285–290 (1953).
14. Bliss, C.I. The toxicity of poisons applied jointly. *Ann. Appl. Biol.* **26**, 585–615 (1939).
15. Parsons, A.B. *et al.* Integration of chemical-genetic and genetic interaction data links bioactive compounds to cellular target pathways. *Nat. Biotechnol.* **22**, 62–69 (2004).
16. Segre, D., DeLuna, A., Church, G.M. & Kishony, R. Modular epistasis in yeast metabolism. *Nat. Genet.* **37**, 77–83 (2005).
17. Borisy, A.A. *et al.* Systematic discovery of multicomponent therapeutics. *Proc. Natl. Acad. Sci. USA* **100**, 7977–7982 (2003).
18. Scott, G.M. & Kyi, M.S. *Handbook of Essential Antibiotics* (Harwood Academic, Amsterdam, 2001).
19. Walsh, C. *Antibiotics: Actions, Origins, Resistance* (American Society for Microbiology, Washington, D.C., 2003).
20. Hoffman, L.R. *et al.* Aminoglycoside antibiotics induce bacterial biofilm formation. *Nature* **436**, 1171–1175 (2005).
21. Perlman, Z. *et al.* Multidimensional drug profiling by automated microscopy. *Science* **306**, 1194–1198 (2004).
22. Hecht, S.M. Bleomycin: New perspectives on the mechanism of action. *J. Nat. Prod.* **63**, 158–168 (2000).
23. Gardner, T.S., di Bernardo, D., Lorenz, D. & Collins, J.J. Inferring genetic networks and identifying compound mode of action via expression profiling. *Science* **301**, 102–105 (2003).
24. Swinney, D.C. Biochemical mechanisms of drug action: what does it take for success? *Nat. Rev. Drug Discov.* **3**, 801–808 (2004).
25. Milo, R. *et al.* Network motifs: Simple building blocks of complex networks. *Science* **298**, 824–827 (2002).
26. Shen-Orr, S.S., Milo, R., Mangan, S. & Alon, U. Network motifs in the transcriptional regulation network of *Escherichia coli*. *Nat. Genet.* **31**, 64–68 (2002).
27. Barabasi, A.L. & Oltvai, Z.N. Network biology: Understanding the cell's functional organization. *Nat. Rev. Genet.* **5**, 101–113 (2004).
28. Remold, S.K. & Lenski, R.E. Pervasive joint influence of epistasis and plasticity on mutational effects in *Escherichia coli*. *Nat. Genet.* **36**, 423–426 (2004).
29. Balaban, N.Q., Merrin, J., Chait, R., Kowalik, L. & Leibler, S. Bacterial persistence as a phenotypic switch. *Science* **305**, 1622–1625 (2004).
30. Komarova, N.L. & Wodarz, D. Drug resistance in cancer: Principles of emergence and prevention. *Proc. Natl. Acad. Sci. USA* **102**, 9714–9719 (2005).